HHS Public Access

Author manuscript

Adv Neurodev Disord. Author manuscript; available in PMC 2018 September 01.

Published in final edited form as:

Adv Neurodev Disord. 2017 September ; 1(3): 176–189. doi:10.1007/s41252-017-0029-1.

Auditory processing enhancements in the TS2-neo mouse model of Timothy Syndrome, a rare genetic disorder associated with autism spectrum disorders

Amanda R. Rendall[*,1], **Aiden L. Ford**[1], **Peter A. Perrino**[1], and **R. Holly Fitch**[1]

[1]Department of Psychology/Behavioral Neuroscience and Institute for Systems Genomics, University of Connecticut, 406 Babbidge Road, Unit 1020, Storrs, CT 06269

Introduction

Autism Spectrum Disorder (ASD) is a set of neurodevelopmental disorders characterized by a complex behavioral phenotype, encompassing deficits in both social and cognitive domains. The core symptoms are heterogeneous, and range from atypical social interactions and language impairments to repetitive behaviors (American Psychiatric Association, 2013). To date, causal mechanisms underlying ASD remain poorly understood, but likely include a complex combination of polygenic and environmental risk factors (Moreno-De-Luca, 2013).

There is a strong genetic influence in ASD, with heritability rates ranging from 70-90% (Bailey et al., 1995; Rosenberg et al., 2009; Steffenburg et al., 1989). However, much is still unknown about the genetic contribution. It is suggested that over a 1,000 genes are involved in ASD, reflecting a complex genetic architecture (DeRubeis et al., 2014). Notably, most of the genes identified have been shown to play a critical role in neurodevelopment, and in fact converge onto several core functional pathways. These can be roughly divided into two major categories: synaptic transmission and excitation/inhibition imbalance; and gene expression involved in transcription/translation (Bourgeron, 2015, for review; Ey, Leblond & Bourgeron, 2011). This is consistent with evidence that genetic mutations associated with ASD influence the structure and the turnover of synapses at different levels, including increasing or decreasing synaptic strength or numbers. Disruption of synapses and signal transmission that alters neuronal connectivity in the brain could in turn mediate functional changes associated with ASD (Auerbach, Osterweil & Bear, 2011; Hahamy, Behrmann, & Malach, 2015). Recent pathway network analyses, coupled with genome-wide association studies of autism, reveal the calcium signaling pathway to be the most affected, suggesting that it is highly involved in the molecular basis of ASD (Skafidas et al., 2014; Wen, Alshikho & Herbert, 2016; Wittkoski et al., 2014). Genes associated with calcium channels modulate neuronal function by mediating influx of calcium into neurons (and thus

[*]Corresponding author: Amanda R. Rendall, University of Connecticut, 406 Babbidge Road, Unit 1020, Storrs, CT 06269. U.S.A. Telephone: (860) 486-3910, Fax: (860) 486-2760, Amanda.Rendall@uconn.edu.

Authors Contributions: AR designed and executed the study, conducted data analyses, and drafted the article. AF assisted with the design, acquisition of data, played a major role in histology and collecting white matter data. PP assisted with collection of behavioral data. HF designed the study and provided critical revisions to the article.

neurotransmitter release), intracellular signaling, and gene transcription. Disruption to any of these can interfere with the neurodevelopmental trajectory.

Among identified ASD risk genes, calcium voltage-gated channel subunit alpha1 C (*CACNA1C*) has been associated with disorders such as bipolar disorder, schizophrenia, major depression, and more recently ASD (Bhat et al., 2012, for review; Li et al., 2015). A single *de novo* missense mutation to the 8A exon of *CACNA1C* gene (which codes for the voltage-gated L-type Ca2+ channel (Cav1.2)) results in a rare multisystem disorder known as Timothy syndrome (TS) (Splawski et al. 2004). This mutation sharply reduces calcium channel inactivation, which may lead to heightened Ca2+ influx (Barrett & Tsien, 2008; Splawski et al., 2004). TS is strongly associated with cardiac arrhythmias, ASD, and neurological dysfunctions that include language impairments, seizures and intellectual disability. All individuals with TS exhibit proarrhythmic prolongation of the cardiac action potential, which generally results in sudden cardiac death at a young age (Splawski et al. 2004). Therefore, it has been challenging to study the basic mechanism of TS in humans, including how this mutation leads to a high co-morbidity with ASD. A genetically engineered knock-in mouse with a heterogeneous TS2 (G406R) mutation in the L-type calcium channel containing a neomycin resistance cassette was developed to study this condition (Bader et al., 2011). The resulting mouse model (TS2-neo knock-in) provides a platform to investigate the role of calcium channel inactivation and calcium signaling in atypical brain development, and in the expression of ASD-like behaviors. Previous behavioral studies on TS2-neo mice found that these animals' exhibit normal general health and anxiety levels, but display a strong autistic phenotype indicated by restricted and repetitive behaviors, altered social behavior, and decreased ultrasonic vocalizations (Bader et al., 2011; Bett et al., 2012).

Understanding the causes of ASD will allow for earlier detection and more refined intervention. However, efforts have been hindered by the heterogeneity and complicated genetic and environmental influences implicated. The study of transgenic mouse models allows us to assess the role of individual genes in modulating biological and behaviorally phenotypes relevant to ASD. Numerous mouse models targeting ASD risk genes have been used to behaviorally phenotype core symptoms of ASD, and particularly repetitive and abnormal social behaviors. One area that has *not* been well explored involves “splinter skills,” or enhanced discrimination of local details within perceptual information among individuals with ASD (Bertone et al. 2005; Plaisted et al. 2003). Superior performance in ASD individuals has been shown in low-level visual perceptual tasks such as visual search (O'Riordan, Plaisted, Driver, & Baron-Cohen, 2001; Plaisted, O'Riordan, & BaronCohen, 1998) and discrimination tasks (Plaisted et al., 1998). Also seen are specific enhancements in pitch discrimination among those with ASD (Bonnel et al. 2010, 2003; Eigsti & Fein, 2013; Heaton and Heaton 2003, 2005; Jones et al. 2009; O'Riordan & Plaisted 2001). A more recent study also found superior auditory performance on detecting perceptual features of pitch and timing in individuals with autistic traits (Stewart, Griffiths, Grube, 2015). These aberrant perceptual processing may relate to the core features of ASD, for example social and communication deficits. However, little animal research has focused on the low-level perceptual enhancements seen in ASD, even though they may impact higher-level cognition and behavior.

The purpose of the current study was to behaviorally characterize TS2-neo mice by assessing their performance on a wide variety of behavioral paradigms, including replication of findings that support the TS2-neo as a valid platform for studying ASD-like behavior. In addition to examining core social and repetitive anomalies, we sought to focus on basic perceptual processing in the auditory domain. All subjects underwent various tasks evaluating their motor coordination, auditory processing, social behaviors, and learning and memory. Following behavioral assessment subjects underwent neuroanatomical analysis of white matter tracts, as well as the medial geniculate nucleus (MGN), since these structures are known to be critical to many behaviors that are affected in ASD.

Method

Subjects

Twelve male TS2-neo mice (B6.Cg-Cacna1ct^{m2Itl}/J; stock number 019547) and 12 matched male wild type (WT) controls (C57BL/6J; stock number 000664) were obtained from The Jackson Laboratory (Bar Harbor, ME). The TS2-neo mouse model has the G406R mutation associated with severe Timothy Syndrome (TS2) and an inverted neomycin resistance cassette, all inserted at the end of exon 8 of the CaV1.2 L-type calcium channel locus (*Cacna1c*) (for more detail on the development of the TS2-neo mouse model see Bader et al., 2011; Bett et al., 2012). The TS2-neo mice do not display any gross behavioral abnormalities in vision, olfaction, or motor strength, thus replicating reports by Bett el al., (2012). Subjects were delivered to the University of Connecticut, Department of Psychology in two separate cohorts (Cohort 1: 6 TS2-neo, 6 WT mice; Cohort 2: 6 TS2-neo, 6 WT mice, all mice received at 7 weeks). All subjects were single-housed in standard mouse tubs (12 h/12 h light/dark cycle), with food and water *ad libitum*. All behavioral testing occurred during the light cycle. At the start of testing, animals were between the ages of postnatal day (P) 55 – P57. Procedures were performed blind to Genotype, and in compliance with the National Institutes of Health and University of Connecticut's Institutional Animal Care and Use Committee (IACUC).

Procedure

Rotarod P57-P61

Subjects were assessed at age P57 for sensorimotor ability and motor learning using a rotarod task. All mice were habituated to the rotarod a day prior to testing, where they were placed on a rotating cylindrical drum that was held at a constant speed of 4 rotations per minute. Subjects underwent 4 trials that maxed out at 2 minutes. Testing began the following day with subjects placed on a rotating cylindrical drum that accelerated from 4 to 40 rotations per minute across 2 minutes. Four trials were administered per day, across five consecutive days. Latency to fall from the rotating drum was averaged across the four trials for each day.

Auditory Processing P70 – P105

Subjects then advanced to auditory processing testing, which utilizes a modified pre-pulse inhibition paradigm (see Fitch et al., 2008 for review). Subjects were placed on individual

load-cell platforms (Med Associates, St. Albans, VT) and presented with auditory stimuli generated using RPvdsEx on a Dell Pentium D PC and RZ6 multifunction processor (Tucker Davis Technologies, Alachua, FL). Sounds were amplified using a Niles SI-1260 Integration Amplifier (Niles Audio Corp., Carlsbad, CA) and delivered through powered Yamaha YHT-M100 speakers (Buena Park, CA). The acoustic startle reflex (ASR; a reflexive response elicited by an unexpected, intense stimulus) was recorded by an iMac 7.1 running Acknowledge 4.1, and obtained via the voltage output from each load cell platform through a linear amplifier (PHM-250U; Med Associates, St. Albans, VT) connected to a Biopac MP150 acquisition system (Biopac Systems, Goleta, CA). The modified pre-pulse inhibition paradigm measured differences in ASR to a loud startle-eliciting stimulus (SES; 105dB, 50 ms, broadband white noise burst (1kHz-10kHz)) when presented with or without a preceding acoustic cue. The ASR difference on cued versus uncued trials provided a measure of cue detection and/or discrimination. If the auditory cue was detected, a reduction (attenuation) in the ASR was expected relative to the ASR elicited when the auditory cue was not present (or not detected). This phenomenon was quantified using an “attenuation score” (ATT) that compared the average amplitude of the ASR from the cued trial to the average ASR of the uncued trial ([average cued ASR/average uncued ASR]*100).

Normal Single Tone P70

Animals were initially tested on Normal Single Tone (NST) to measure baseline pre-pulse inhibition and auditory ability (P70). This auditory PPI control task was used to establish whether subjects exhibited hearing deficits and/or impaired gross motor reflexes that could confound other auditory PPI tests, and provided an index of baseline auditory pre-pulse inhibition ability across test groups. Testing sessions consisted of 104 pseudorandomly presented cued and uncued trials at inter-trial intervals (ITI) of varying duration (16–24 s). The task comprised a silent background and a simple single tone cue (50 ms, 75 dB, 8,000 Hz tone) presented 50 ms prior to the 50 ms, 105 dB SES. All subjects were able to perform this task, and therefore were used for further auditory processing evaluation.

Embedded Tone P71-P83

The variable duration Embedded Tone (EBT) task (300 sequential pseudorandom trials) assessed ability to detect a change in tone frequency relative to a standard background tone (cue was a variable duration 5.6 kHz pure tone embedded in a 10.5 kHz background pure tone). On cued trials, the cue was presented 100 ms before the SES, while uncued trials used a “cue” of 0 ms. Two EBT tasks were used in this study – a long-duration EBT (0 ms to 100 ms), and a short-duration EBT (0 ms to 10 ms). A range of cue durations were used to evaluate specific thresholds for performance differences between the genotypes, since groups might perform comparably on longer durations yet differ on shorter durations (which are more difficult to detect). Using a range of cue durations enables ascertainment of stimulus features that all animals can discriminate (ceiling), that no animals can discriminate (basement), as well as any group differences in the mid-range. Both EBT tasks were administered for five consecutive days (P71-P83).

Silent Gap P86-P98

A Silent Gap (SG) task was used to assess ability to detect silent breaks in continuous white noise (P86 to P98). A session included 300 trials with a continuous 75 dB broadband white noise background, with pseudorandomized cued and uncued trials. On cued trials, a silent gap of variable duration (0-100 ms or 0-10 ms) was presented 100 ms before the SES, while a “0 ms” trial served as the uncued condition. Subjects were tested on the Silent Gap task for five consecutive days using both versions of the task.

Pitch Discrimination P101-P105

Pitch discrimination testing also took place across five consecutive days of testing (300 trials/day). This task assessed ability to detect very small changes in pitch embedded in a background tone. A variable ITI (16–24s) was used, and the cue was a 300 ms, 75 dB tone of variable frequency embedded in a standard 75 dB, 10500 Hz background pure tone (2 ms up/down linear frequency ramp) prior to the SES. The experimental frequencies used for the pitch discrimination task deviated from the standard background frequency by as much as 75 Hz, to as little as 5 Hz. Uncued trials did not include a frequency deviant prior to the SES.

Three-Chamber Social Interaction – P107-P110

The Three-Chamber test was used to assess general sociability as well as social recognition. This test derives from observations that healthy wild-type mice typically prefer to spend time with a conspecific (social stimulus) rather than an object (non-social stimulus). After a 5 min habituation period, the subjects were allowed to freely explore three chambers, with one containing another “stranger” mouse, and another chamber on the opposite side containing a novel object. The subject was placed into the middle (empty) chamber and was able to freely explore all the chambers for 10 min. Next we placed an unfamiliar conspecific mouse (“stranger 2”) where the novel object was previously located, and subjects were given another 10 min to explore the chambers. The percent time spent interacting with the mouse during the social preference phase, and percent time spent interacting with the novel mouse during the social recognition phase, were recorded and analyzed.

Social Dominance – Tube Test P113-P116

The Tube Test was administered to evaluate social dominance/aggression. The tube used for this task was a clear plexiglas tube (length 30.5cm; outer diameter 4.5cm; inner diameter 3.5cm). This narrow space is just sufficient for a mouse to walk through without being able to reverse direction. Mice were trained to walk through the tube before testing. A WT and a mutant mouse were randomly paired on different sides of the tube (balanced), and released at the same time into the tube. The mouse that forced the other mouse to back out of the tube was considered the “winner” of the trial (recorded for analysis). Each mouse underwent 4 trials paired with a different randomly assigned subject and the percentage of wins was calculated and analyzed. Mice were not paired within Genotype since by definition this would yield a score of 50%.

Marble Burying P115-P118

Subjects were placed in a standard polycarbonate cage (26 cm × 48 cm × 20 cm) filled with fresh mouse bedding (5cm deep) for the marble burying test. Standard glass toy marbles (assorted styles and colors, 15 mm diameter, 5.2 g in weight) were placed on the surface of the bedding in 3 rows of 7 marbles. A marble was considered buried if at the end of the 45 minute session the marble was more than half-way covered by bedding. Subjects were given 45 minutes to explore the area; number of marbles buried were reported and used for analysis.

Vocalizations during male-female interactions P122-P126

Adult male vocalizations were recorded during individual male-female pair social interactions. Male mice produce ultrasonic vocalizations when they are in the presence of a female (and particularly during estrus), or when they detect a female's urinary estrus pheromones. We measured the vocalization emission of all subjects when exposed to accumulated seven-day dirty bedding obtained from mature, age-matched C57 female. Bedding from seven-days was used to ensure inclusion of estrus phase (4 day cycle). That same female was free moving in the cage with the male subject during recording. On P122-126 male subjects were individually placed in a standard laboratory cage filled with bedding, dirty bedding and a freely moving female. Only WT females were used to avoid confounds. Vocalizations were recorded for 5 minutes using a 1/4 inch condenser microphone (Brüel & Kjær type 4136, Nærum, Denmark) suspended 10 cm above the test subject. The microphone signal was preamplified with a Brüel & Kjær type 2619 preamplifier and then amplified using a Brüel & Kjær type 2636 amplifier (Brüel & Kjær, Nærum, Denmark). The signal was digitized at a sampling rate of 200 kHz using a Tucker Davis Technologies (Alachua, FL) multifunction processor (RZ6) and saved as a .wav file using a custom MATLAB program (MathWorks, Natick, MA) on a Dell Pentium IV PC. Recorded sound waveforms were visualized and assessed using Adobe Audition (Adobe, San Jose, CA). Total time spent vocalizing was calculated by extracting vocalization intervals (continuous vocalization epochs, 200 ms apart) from periods of silence (no vocalizations). Time spent vocalizing was binned into minute periods across the 5 minute male-female interaction. Since females vocalize little in the presence of males, all recorded vocalizations were presumed to reflect the male subject (D'Amato & Moles, 2001; Moles et al., 2007; Wang et al., 2008).

Water Maze Testing P127-150

Subjects were initially tested on a water escape to assess any underlying impairments that might confound further maze testing (i.e., deficits in motivation, swimming, or visual acuity). Subjects were placed in the far end of an oval tub (103 cm × 55.5 cm) filled with room temperature water, and given 45 seconds to swim to a visible escape platform (8.5 cm in diameter; 1 cm above water surface) at the opposite end of the tub. Latencies to reach the visible platform were recorded. None of the subjects displayed any impairment on this task, and thus all proceeded to Morris water maze testing.

The Morris water maze is a behavioral task commonly used to assess spatial learning and memory, and specifically the ability to locate the position of a submerged escape platform

using extra maze cues. Beginning on P129, subjects were tested on the Morris water maze over a span of five consecutive test days (sessions). During each test session, subjects were given four trials to locate the submerged platform. For each trial, the subject starting location was selected pseudorandomly at one of the four compass locations (i.e. north, south, east, and west), with each location used once per test session. Subjects were allowed 45 seconds to complete the trial and find the escape platform. If the platform was not located at 45-seconds, subjects were gently guided to the goal before removal from the maze. The position of the hidden platform remained static throughout all five test sessions. Latency to the escape platform was measured and recorded using a Sony camera integrated with a SMART video-tracking program (Panlab, Barcelona, Spain).

Subjects then progressed to a water version of the 4/8 radial arm maze (adapted from Hyde, Hoplight & Denenberg, 1998). This task was used to assess spatial reference and working memory ability simultaneously, using a standard 8 arm radial maze with 4 arms baited (i.e., containing a submerged goal platform), and 4 arms open but never baited. Configuration of goal arms were counterbalanced between subjects but remained fixed per subject across all sessions. Additionally, high contrast extra-maze cues were present, and the locations of these remained static for the experiment.

The day prior to testing (Day 1), subjects were given a training session where all arms that would not contain a platform were blocked, forcing the animals to only enter arms containing a platform. Subjects were placed in the start arm and given 120 seconds to locate a platform. Every subject completed 4 training trials, and each time they found a platform, that platform was removed and the entrance to that arm was blocked. This ensured that the subject could no longer enter this arm for the remainder of the training session. If the subject failed to find a platform in this window, they were guided to the nearest available goal. Once on the platform, subjects remained for 20 seconds and then were removed from the maze to their home cage (30 second inter-trial interval; ITI).

Testing began on Day 2 and continued for an additional 14 consecutive days. Here, instead of blocking the goal arm of the most recently located platform, the platform was removed during the 30 second ITI. However, the arm remained open and unbaited for the remainder of the test session. Animals were required to locate all 4 platforms, and thus received 4 test trials per day. Test sessions were recorded using a Sony camera integrated with the SMART video-tracking program (Panlab, Barcelona, Spain). Total number of errors were recorded and used for analysis.

Perfusion and histology P191

At the completion of testing, all 24 subjects were weighed, anesthetized using ketamine (100mg/kg) and xylazine (15 mg/kg), and transcardially perfused using a .09% saline solution with formalin as the fixative. Brains were extracted and stored in formalin to postfix at 4°C. Sixteen tissue samples (8 TS2-neo, 8 WT) were stored long-term to await neuroanatomic assessment using a Nissl stain (with remaining tissue used in other immunohistochemical analyses).

Formalin-fixed brains were serially sectioned in the coronal plane at 60 μm using a vibratome (Leica VT1000 S). Every second section was mounted on gelatin-subbed slides and stained for Nissl bodies using cresyl violet (coverslipped with DPX mounting medium).

Volumetric measures of white matter structures were assessed, including corpus callosum, cingulum, external and internal capsule, fornix, and anterior commissure. All prepared samples were analyzed using the Stereo Investigator System (MBF Biosciences, Williston, VT, USA) integrated with a Zeiss Axio Imager A2 microscope (Carl Zeiss, Thornwood, NY). For all structures, volumes were reconstructed from serial area scores using the Cavalieri Estimator probe in *StereoInvesigator*. Neuronal cell populations were estimated using the Optical Fractionator probe, with cross sectional neuronal cell area estimated concurrently using the Nucleator probe. Neurons were only counted for analysis if the nucleolus was in focus and within the appropriate boundaries of the active counting frame and dissector depth. A standard stereotaxic atlas was used to determine the borders of the MGN for quantification (Lein et al., 2007; Paxinos & Watson, 1986). An average of 8 to 10 sections per brain was used for white matter tract analysis while an average of 6 sections per brain was used for MGN analysis. Volumetric measurements as well as contours of the MGN were drawn at 2.5× magnification. Cell size measurements and counts were assessed at 100X magnification. A sampling grid size of 200 μm × 200 μm and a 30 μm × 30 μm counting frame were used for stereological examination. Estimates for both neuronal cell population and neuronal cell area were obtained for left MGN, right MGN, and total (left + right) MGN for each subject. All measurements were performed blind to genotype.

Data Analyses

All subjects were used for analysis (WT, n = 12; TS2-neo, n = 12). Group differences on rotarod performance were analyzed using a 2 (Genotype; TS2-neo and WT) × 5 (Day) repeated measures analysis of variance (ANOVA). Normal Single Tone (baseline control) data was examined using a univariate ANOVA comparing TS2-neo and WT attenuation scores. Although, there were no significant differences in performance on NST, NST attenuation scores were used as a covariate in subsequent statistical analysis to control for individual variations in baseline auditory prepulse inhibition (PPI). Differences in attenuation (ATT) scores during all auditory tasks (embedded tone, silent gap and pitch discrimination) were examined using a 2 × 5 × 9 repeated measures ANOVA with Genotype (2 levels: TS2-neo and WT) as the between-subjects variable, and Day (5 levels) and cue (9 levels) as the within-subjects variable. A univariate ANOVA was performed to analyze differences between Genotypes on the following tasks, social interaction, social dominance tube task, marble burying, vocalizations and water escape. A repeated measures ANOVA was performed to analyze latency to platform in the Morris water maze with Day (5 levels) being the within-subject variable and Genotype being the between subjects variable. Average total errors were examined for the 4/8 radial water maze, using a 2 × 14 repeated measures ANOVA, with Genotype (2 levels: TS2-neo and WT) as the between measure and Days (14 levels) as the within measure. For neuroanatomical measures, subjects in the Nissl stained group (n=16, 8 TS2-neo/8 WT) were used for analysis. Group differences in regional volume and cellular measurements (mean cell count and size within defined boundaries) were assessed using a univariate ANOVAs. Examination of cell size distribution was

conducted using a cumulative percent distribution. To examine group differences in cell size distribution, non–parametric analyses with Kolmogorov Smirnov (K-S) tests were conducted on the cumulative percent distributions of each Genotype. A bivariate correlation was used to examine the relationship between number of neurons and auditory processing performance. All statistical analyses were conducted using SPSS 19 with an alpha criterion of 0.05, two-tailed.

Results

Rotarod

A repeated measures ANOVA examining average rotarod latency across 5 days of testing revealed a main effect of Genotype [$F(1,22) = 14.037$, $p<.05$], as well as a Genotype × Day interaction [$F(4,88) = 8.251$, $p<.001$]. TS2-neo mice showed impaired sensorimotor/motor ability, and the lack of improvement across days indicates they failed to show motor learning on this task (Fig. 2a).

Auditory Processing

All subjects were initially tested on a normal single tone (NST) task, to establish baseline hearing and PPI ability. None of the subjects showed impairments on NST, nor was there a main effect of Genotype [$F(1,22) = .392$, $p>.05$]. We did however controlled for individual variations in baseline auditory prepulse inhibition (PPI) performance using NST attenuation scores as a covariate. On the embedded tone (EBT) 0-100 ms task, we found no main effect of Genotype [$F(1,21) =1.394$, $p>.05$] (Fig 3a), and all subjects were able to discriminate the stimuli based on cued/uncued amplitude comparisons. On the more difficult embedded tone task (cue durations ranging from 0 to 10 ms, where 0 ms is the uncued condition) we found a main effect of Genotype [$F(1,21) = 5.388$, $p<.05$], with TS2-neo mice showing *enhanced* detection of the embedded tone cue compared to WTs (Fig. 3b). For silent gap detection we assessed performance on the 0-300 ms task, and again saw no main effect of Genotype [$F(1,21) = .004$, $p>.05$] (Fig. 3c). On the silent gap 0-100 ms task, we found overall worse performance (since the task was harder), and also a main effect of Genotype [$F(1,21) = 7.369$, $p<.05$], with TS2-neo mice again demonstrating *superior* performance on gap detection (Fig. 3d). On the pitch discrimination task, we did not find a main effect of Genotype [$F(1,21) = .731$, $p>.05$].

Three-Chamber Social Interactions

On the three-chamber social interaction tasks we did not find a main effect of Genotype, either in the social preference phase [$F(1,22) = 1.426$, $p>.05$], nor the social recognition phase [$F(1,22) = .001$, $p>.05$]. On all tasks, WTs and TS2-neo mice spent a comparable percentage of time exploring the social stimuli (Fig. 1d).

Social Dominance

On the social dominance (tube task) the number of wins was calculated as a percentage of the 4 trials. We found a main effect of Genotype [$F(1,22) = 12.138$, $p<.01$], with TS2-neo mice showing more “wins” compared to WT controls. These findings indicate TS2-neo's were more aggressive (Fig. 1a).

Marble Burying

A univariate ANOVA revealed a main effect of Genotype [$F(1,220 = 10.662$, $p<.01$] on the marble burying task with TS2-neo mice burying significantly more marbles compared to WTs. This indicates the mutants expressed more stereotyped and repetitive behaviors (Fig. 1c).

Vocalizations

A univariate ANOVA was conducted to evaluate time spent vocalizing for each minute spent interacting with a female mouse. Analysis revealed that TS2-neo mice vocalized significantly less during male-female interactions after the initial two minutes, [Minute 1: $F(1,22) = .187$, $p>.05$; Minute 2: $F(1,22) = .180$, $p>.05$; Minute 3: $F(1,22) = 4.803$, $p<.05$; Minute 4: $F(1,22) = 4.058$, $p<.10$; Minute 5: $F(1,22) = 6.498$, $p<.05$] (Fig. 1b).

Water Maze Testing

Prior to spatial water maze testing, a visible platform control task was conducted to assess any underlying impairments that could confound subsequent water maze performance (e.g., impairments in swimming ability, visual acuity, or motivation). A univariate ANOVA on latencies found no main effect of Genotype [$F(1,22) = .037$, $p>.05$] indicating that genetically modified groups had no impairments on underlying aspects of the water task (e.g., swimming)

On the Morris Water Maze task we found no main effect of Genotype [$F(1,22) = .013$, $p>.05$], but did find a main effect of Day [$F(4,88) = 6.313$, $p<.01$], with all subjects showing decreased latencies as testing progressed (indicating learning; Fig. 2b). This indicated learning for all subjects.

The 4/8 radial arm water maze was used to simultaneously measure spatial working and reference memory performance. A repeated-measures analysis of the average number of total errors (working memory, initial reference, and repeated reference memory errors) revealed no significant difference between WT and TS2-neo groups [$F(1,22)=.016$, $p>.05$] (Fig. 2c). A main effect of Day [$F(13,286)=5.348$, $p<.01$] was observed, confirming that both groups reduced errors across days (i.e., showed learning). We also examined group differences in error types including working memory, initial reference memory, and repeated reference memory. Again repeated measures ANOVA reveal no effect of Genotype on any error types (working memory [$F(1,22)=.098$, $p=.757$], initial reference memory [Genotype: $F(1,22)=.00$, $p>.05$] and repeated reference memory [Genotype: $F(1,22)=.574$ $p>.05$]).

White matter tract volumes

Initial analysis of white matter tract volumes (Nissl stained samples, n=16 (8 TS2-neo/8 WT)), revealed a main effect of Genotype for volume of external capsule volume, with TS2-neo mice showing significantly smaller external capsule volumes compared to WTs[$F(1,16)=6.417$, $p<.05$]. A subsequent examination of hemisphere-dependent effects showed that this decrease was localized to the right external capsule [$F(1,16)=10.737$ $p<.01$]. Analysis of total fornix volume also showed a trend towards reduced volume in the TS2-neo

group [F(1,16)=4.209, p<.1] (Figure 4). No Genotype differences were seen for other white matter structures assessed.

Medial Geniculate Nucleus

A univariate ANOVA comparing MGN volume revealed a marginal main effect of Genotype, with a smaller MGN volume in TS2-neo mice compared to WTs [F(1,14) = 4.250, p=.058] (Fig. 5a). Examination of mean cell size in the MGN found no main effect of Genotype [F(1,14) = .384, p>.05]. However, comparisons of cumulative percent distributions between TS2-neo and WT controls using a Kolmogorov Smirnov test revealed a significant K-S statistic (p<.05; Fig. 5b). Analysis of cell size distribution in TS2-neo and WT brains revealed that TS2-neo brains contain more small and fewer large MGN cells than controls. A univariate ANOVA comparing MGN neuronal population revealed a main effect of Genotype, specifically for the right MGN, with TS2-neo mice exhibiting fewer neurons compared to WTs [total: F(1,14) = 2.489, p>.05; left: F(1,14) = .180, p>.05; right: F(1,14) = .045, p<.05] (Fig.5c). A bivariate correlation revealed a significant positive relationship between neuronal population in the MGN and average attenuation scores on EBT 0-10 in TS2-neo mice only (r = .792 n = 8, p<.05) (Fig. 5d). Specifically, an increase in the number of neurons in the MGN was correlated with an increase in attenuation score (*worse* performance) on the EBT 0-10 task. This relationship was not seen in the WTs (r = -.269, n= 8, p>.05) or on any other auditory processing task.

Discussion

The purpose of this study was to behaviorally evaluate TS2-neo mice on motor learning, auditory processing, social and repetitive behaviors, as well as, on learning and memory tasks. Results showed that the loss of Ca.V1.2 inactivation in this mouse model significantly affected motor learning, auditory processing, and social and repetitive behaviors, but did not impact on spatial learning and memory. Additionally, structural anomalies were seen for mutant mice in some white matter tracts, and MGN.

TS2-neo serves as a model of ASD

The results presented here reaffirm that when TS mutant channels are expressed at reduced levels (but low enough to avoid fatality), effects include behaviors consistent with symptoms observed in the clinical ASD population. Specifically, we found that the TS2-neo mice displayed deviant social behaviors, as well as repetitive behaviors replicating what has previously been reported in TS2-neo mice (Bader et al., 2011). Effects were also seen on a social dominance task, with mutants winning significantly more trials compared to their WT controls (thus showing more aggressive behavior). However, we did not observe any differences in social preference or recognition on the three-chamber task. This is actually consistent with Bader et al., (2011), where no differences in sociability measures were seen between TS2-neo and WT mice during the first 10 min of the task. In fact, Bader et al., (2011) only found differences in social behavior by testing over an unusually extensive period (a few hours, which is non-standard for the 3-chamber task). Also, our subjects were given the option to explore a novel inanimate object, rather than an empty chamber (as used by Bader et al.). These discrepancies in protocols may explain why we did not observe

Genotype differences in social behavior on this task. However, we found that TS2-neo subjects spent significantly less time vocalizing to a female in a vocalization task. Importantly, Bader et al., (2011) previously observed reduced vocalizations in pups, but not adults. Our findings show that aberrant social and communicative behaviors persist into adulthood, and across different types of social interactions. Lastly, subjects underwent a marble burying task, which we showed that TS2-neo mice buried twice as many marbles compared to their controls. This excessive burying is further indicative of repetitive, restricted and perseverative behavior -- another core symptom of ASD. Overall, these findings replicate prior reports on the TS2-neo model (Bader at al., 2011), and affirm that this mouse model exhibits core ASD-like traits such as repetitive behaviors and altered social behavior and ultrasonic vocalizations.

Motor and Spatial Learning

In addition to phenotyping core behavioral symptoms of ASD, we evaluated the TS2-neo mice on both motor and spatial learning. Although not a core criterion, motor and procedural learning deficits have been noted in individuals with ASD and it is thought that deficits in procedural learning may contribute to the cognitive and behavioral phenotype of autism. Here, the TS2-neo mice showed deficits in motor coordination and motor learning, as indicated by a lack of improvement across days on the Rotarod task. There have been parallel reports of impairments in motor coordination in ASD populations across a wide range of behaviors (Fournier et al., 2010). Furthermore, it has also been reported that children with ASD demonstrate diffusely decreased connectivity across the motor execution network relative to control children (Mostosky et al., 2009). This cortico-cerebellar connectivity dysfunction is also considered a core characteristic of ASD, and is thought to contribute to anomalies in both sensory-motor control, and higher function such as social cognition and emotion (Crippa et al., 2016).

Finally, for spatial learning and memory in TS2-neo mice, we found no differences between Genotypes on either the Morris water maze or the 4/8 radial arm water maze. Similarly, Bader et al, (2011) evaluated TS2-neo mice on the Morris water maze and found no differences in learning. However, they did report that TS2-neo mice perseverated to the previous learned quadrant during a reversal task, suggesting that TS2-neo mice display comparable initial learning but are cognitively *inflexible* when given a reversal task. Our results here replicate initial findings as well as exemplify that TS2-neo mice can perform adequately on a complex spatial reference and working memory task as seen on the 4/8 radial arm water maze.

Auditory Processing Enhancements

The current study revealed novel findings that TS2-neo mice displayed *superior* performance on both the embedded tone and silent gap task for short cue durations. Enhanced low-level perceptual discrimination has been reported in individuals with ASD for visual and auditory stimuli (Bertone et al., 2005; Mottron et al., 2006; Plaisted et al., 2003), and this is the second ASD-like mouse model our lab has reported to display enhanced performance on an auditory processing task. Specifically, we previously found that *Cntnap2* KO mice displayed superior discrimination on an embedded tone and pitch discrimination task (Truong et al.,

2015). Interestingly, this type of superiority in auditory processing is not seen in other mutant rodent models, for example knock-outs using candidate susceptibility dyslexia risk genes (Rendall et al., 2015; Truong et al., 2014; Szalkowksi et al., 2013; Szalkowksi et al., 2012). Thus although low-level superiority in auditory processing may be related to language deficits seen in ASD (Eigsti & Fein, 2013), these same superiorities do not seem to occur in other language-specific developmental disorders (e.g., dyslexia and specific language impairment). As such, low-level auditory enhancements form a particularly interesting aspect of the ASD-like animal model profile. An additional new finding --that better performance on the EBT 0-10 task (on which we have reported a similar atypical superiority in another ASD mouse model, Cntnap2; Truong et al., 2015) is actually correlated to *fewer* neurons in the MGN (which has generally been associated with deficits including language anomalies; Galaburda, Menard, & Rosen, 1994) – may further support the notion that low-level sensory *enhancements* are directly related to auditory-based language *impairments* in at least a subset of individuals with ASD. Further research should investigate other well-established mouse models of ASD by focusing on auditory processing patterns, to see if this trend of superior auditory processing is ubiquitous across multiple ASD mouse models beyond the TS2-neo and *Cntnap2* KO mice, and whether the relationship with anomalous MGN cellular morphology can be replicated.

Genetic, neurodevelopmental and behavioral exploration of these enhancements is important because low-level perceptual abilities are particularly important for the development of language, and differences in processing may be contributing to core features of autism such as language delay and aberrant social skills. In fact, atypical auditory processing in children with autism may be key to parsing different etiologies of autism, establishing interventions, and ameliorating overwhelming auditory sensory input to facilitate language development.

Enhanced perceptual functioning and cortico-cortical disconnection theories

The behavioral phenotype validated in the TS2-neo mouse model also aligns with the enhanced perceptual functioning theory of ASD put forth by Mottron et al. (2006). These authors contend that the paradoxical co-occurrence in ASD of enhanced sensory perceptual abilities and compromised global sensory integration (including social and language deficits) might be explained by a developmental re-orientation of cortical functional patterns. Specifically, locally oriented “low-level” processing mechanisms may be enhanced and favored over more complex, integrative strategies that engage global and long-range processing mechanisms. This may further relate neurocognitively to regional hyper-connectivity and long-range hypo-connectivity (discussed further below).

Atypical white matter development in the TS2-neo

A growing body of neuroimaging studies identifies abnormal development of white matter tracts and organization of grey matter structures as markers of an ASD neurostructural phenotype, which we saw reflected in our own results. In the current study, we report reductions in volumes of the external capsule and fornix, two major white matter tracts. The external capsule contains cortico-cortical association fibers that form the basis of intercortical communication between the basal forebrain and other regions of the cerebral cortex, while the fornix is a bundle of commissural fibers connecting the hippocampus,

mammillary bodies, and thalamus between the two hemispheres of the brain. Our findings of reductions in the fornix parallel reported results from neuroanatomical studies of the BTBR and NL3 mouse models of ASD, which showed decreases in fornix volume and integrity (Ellegood et al., 2015). Collectively, these results contribute to the larger body of work assessing ASD as a disorder of hypo-connectivity and disconnection between fronto-cortical and cortico-cortical networks. These pathways are critical for the integration of information that promotes normative socio-communicative development and deficits in connection integrity and structure are correlated with ASD symptom severity (Alexander et al., 2007; Poustka et al., 2012). This pattern of aberrant white matter development in ASD has become so consistent that some suggest that with further research it could become a unifying neuro-endophenotype for ASD.

TS2-neo mice display alterations within the MGN

Stereological analysis of the MGN revealed a reduction in MGN volume and number of neurons as well as neuronal size distribution shift toward more small neurons in TS2-neo mice relative to WTs. Furthermore, a significant correlation was observed between number of neurons and mean EBT10 performance in TS2-neo mice only. Co-occurrence of these findings suggests that aberrant MGN morphology is related to enhanced auditory processing phenotype, as observed in TS2-neo mice on EBT 0-10. These findings are consistent with *in vivo* neuroimaging studies showing fundamental differences in the thalamus of ASD individuals, including reduced volume (Tamura et al., 2010; Tsatsanis et al., 2003), altered neurochemical composition (Friedman et al., 2003), and abnormal thalamocortical connectivity (Chen et al., 2016; Cheon et al., 2011; Chugani et al., 1997; Mizuno, Villalobos, Davies, Dahl, & Muller, 2006; Muller et al., 1998; Nair et al., 2013). This collective evidence suggests that the thalamus may play a particular role in the etiology of ASD symptoms. TS2-neo neuroanatomical differences appear to be more robust within the right hemisphere, which corresponds to prior reports that TS2-neo brains are significantly more asymmetric than littermates (Bett et al., 2012). Further research is necessary to understand how alterations within the MGN may be contributing to the auditory enhancements observed, and in particular, why and how a reduction in the number of neurons and neuronal size could be advantageous to auditory processing but detrimental to language development.

Transgenic mouse models serve as a critical tool in evaluate the role of individual genes in the complex and polygenic cascade underlying neurodevelopment, and can further help to reveal how single-gene mutations can disrupt this process and result in neurodevelopment disorders (e.g., ASD). Among ASD genes identified, ~ 200 have been used to create engineered mouse models, and associated phenotyping studies have revealed atypical social and perseverative/repetitive behaviors (3-chamber task, marble burying, alternating choice, task reversal) that can be linked to various disruptions in specific gene function (see Crawley, 2004 for review). Although major strides have been made in mapping the genetic etiology of ASD-like deficits in the social and repetitive domains, few studies have used transgenic mice to delineate some of the low-level enhancements associated with ASD. Yet these features may prove to be critical in unravelling neurogenetic influences on the higher-order language and communication deficits associated with ASD. Indeed, while several

prominent research groups in the field have successfully associated ASD risk gene mutations with decreases in vocal calls and/or atypical call acoustics (Ey et al., 2013, Lai et al., 2014, Michetti, Ricceri & Scattoni, 2012; Penagarikano et al., 2011; Penagarikano & Geschwind, 2012), little animal work has focused on core perceptual and sensory processing features that may contribute to higher order anomalies. Here we have demonstrated an association between enhancements in low-level acoustic processing and a TS2-neo mutation associated with an ASD profile, bolstering prior data showing similar features in a *Cntnap2* KO mouse model of ASD. Ongoing research to examine perceptual processing, including such enhancements, in ASD models will continue to benefit our understanding of the neurogenetic etiology of this complex disorder.

Supplementary Material

Refer to Web version on PubMed Central for supplementary material.

Acknowledgments

This research was supported by **NSF IGERT Grant 1144399** to the University of Connecticut (J. Magnuson, PI), by the **Murine Behavioral Neurogentic Facility** (MBNF) at the University of Connecticut and by the **National Institutes of Health grant P01HD057853** to R.H. Fitch.

References

Alarcón M, Abrahams BS, Stone JL, Duvall JA, Perederiy JV, Bomar JM, et al. Nelson SF. Linkage, association, and gene-expression analyses identify *CNTNAP2* as an autism-susceptibility gene. The American Journal of Human Genetics. 2008; 82(1):150–159. [PubMed: 18179893]

Alexander AL, Lee JE, Lazar M, Boudos R, DuBray MB, Oakes TR, et al. Diffusion tensor imaging of the corpus callosum in Autism. Neuroimage. 2007; 34:61–73. [PubMed: 17023185]

American Psychiatric Association. Diagnostic and statistical manual of mental disorders. 5th. Arlington, VA: American Psychiatric Publishing; 2013.

Auerbach BD, Osterweil EK, Bear MF. Mutations causing syndromic autism define an axis of synaptic pathophysiology. Nature. 2011; 480(7375):63–68. [PubMed: 22113615]

Bader PL, Faizi M, Kim LH, Owen SF, Tadross MR, Alfa RW, et al. Shamloo M. Mouse model of Timothy syndrome recapitulates triad of autistic traits. Proceedings of the National Academy of Sciences. 2011; 108(37):15432–15437.

Bailey A, Le Couteur A, Gottesman I, et al. Autism as a strongly genetic disorder: evidence from a British twin study. Psychological Medicine. 1995; 25(1):63–77. [PubMed: 7792363]

Barrett CF, Tsien RW. The Timothy syndrome mutation differentially affects voltage-and calcium-dependent inactivation of CaV1. 2 L-type calcium channels. Proceedings of the National Academy of Sciences. 2008; 105(6):2157–2162.

Bertone A, Mottron L, Jelenic P, Faubert J. Enhanced and diminished visuo-spatial information processing in autism depends on stimulus complexity. Brain. 2005; 128(10):2430–2441. [PubMed: 15958508]

Bett GC, Lis A, Wersinger SR, Baizer JS, Duffey ME, Rasmusson RL. A mouse model of Timothy syndrome: A complex autistic disorder resulting from a point mutation in Cav1. 2. North American journal of medicine & science. 2012; 5(3):135. [PubMed: 24371506]

Bhat S, Dao DT, Terrillion CE, Arad M, Smith RJ, Soldatov NM, Gould TD. CACNA1C (Ca v 1.2) in the pathophysiology of psychiatric disease. Progress in neurobiology. 2012; 99(1):1–14. [PubMed: 22705413]

Bonnel A, Mottron L, Peretz I, Trudel M, Gallun E, Bonnel AM. Enhanced pitch sensitivity in individuals with autism: A signal detection analysis. Journal of cognitive neuroscience. 2003; 15(2):226–235. [PubMed: 12676060]

Bonnel A, McAdams S, Smith B, Berthiaume C, Bertone A, Ciocca V, et al. Mottron L. Enhanced pure-tone pitch discrimination among persons with autism but not Asperger syndrome. Neuropsychologia. 2010; 48(9):2465–2475. [PubMed: 20433857]

Bourgeron T. From the genetic architecture to synaptic plasticity in autism spectrum disorder. Nature Reviews Neuroscience. 2015; 16(9):551–563. [PubMed: 26289574]

Chen H, Uddin LQ, Zhang Y, Duan X, Chen H. Atypical effective connectivity of thalamo-cortical circuits in autism spectrum disorder. Autism Research. 2016; 9(11):1183–1190. [PubMed: 27868393]

Cheon K, Kim Y, Oh S, Park S, Yoon H, Herrington J, et al. Schultz RT. Involvement of the anterior thalamic radiation in boys with high functioning autism spectrum disorders: A diffusion tensor imaging study. Brain Research. 2011; 1417(0):77–86. [PubMed: 21890117]

Chugani DC, Muzik O, Rothermel R, Behen M, Chakraborty P, Mangner T, et al. Chugani HT. Altered serotonin synthesis in the dentatothalamocortical pathway in autistic boys. Annals of Neurology. 1997; 42(4):666–669. [PubMed: 9382481]

Crawley JN. Designing mouse behavioral tasks relevant to autistic-like behaviors. Mental retardation and developmental disabilities research reviews. 2004; 10(4):248–258. [PubMed: 15666335]

Crippa A, Del Vecchio G, Ceccarelli SB, Nobile M, Arrigoni F, Brambilla P. Cortico-Cerebellar Connectivity in Autism Spectrum Disorder: What Do We Know So Far? Frontiers in psychiatry. 2016; 7:20. [PubMed: 26941658]

D'Amato FR, Moles A. Ultrasonic vocalizations as an index of social memory in female mice. Behavioral neuroscience. 2001; 115(4):834. [PubMed: 11508722]

De Rubeis S, Buxbaum JD. Genetics and genomics of autism spectrum disorder: embracing complexity. Human molecular genetics. 2015; 24(R1):R24–R31. [PubMed: 26188008]

Di Martino A, Yan CG, Li Q, Denio E, Castellanos FX, Alaerts K, et al. Deen B. The autism brain imaging data exchange: towards a large-scale evaluation of the intrinsic brain architecture in autism. Molecular psychiatry. 2014; 19(6):659–667. [PubMed: 23774715]

Eigsti IM, Fein DA. More is less: pitch discrimination and language delays in children with optimal outcomes from autism. Autism Research. 2013; 6(6):605–613. [PubMed: 23929787]

Ellegood J, Anagnostou E, Babineau BA, Crawley JN, Lin L, Genestine M, et al. Clustering autism: using neuroanatomical differences in 26 mouse models to gain insight into the heterogeneity. Molecular Psychiatry. 2015; 20:118–125. [PubMed: 25199916]

Ellegood J, Babineau BA, Henkelman RM, Lerch JP, Crawley JN. Neuroanatomical analysis of the BTBR mouse model of autism using magnetic resonance imaging and diffusion tensor imaging. NeuroImage. 2013; 70:288–300. [PubMed: 23275046]

Ey E, Leblond CS, Bourgeron T. Behavioral profiles of mouse models for autism spectrum disorders. Autism Research. 2011; 4(1):5–16. [PubMed: 21328568]

Ey E, Torquet N, Le Sourd AM, Leblond CS, Boeckers TM, Faure P, Bourgeron T. The Autism ProSAP1/Shank2 mouse model displays quantitative and structural abnormalities in ultrasonic vocalisations. Behavioural brain research. 2013; 256:677–689. [PubMed: 23994547]

Fitch RH, Threlkeld SW, McClure MM, Peiffer AM. Use of a modified prepulse inhibition paradigm to assess complex auditory discrimination in rodents. Brain research bulletin. 2008; 76(1):1–7. [PubMed: 18395604]

Foss-Feig JH, Kwakye LD, Cascio CJ, Burnette CP, Kadivar H, Stone WL, Wallace MT. An extended multisensory temporal binding window in autism spectrum disorders. Experimental Brain Research. 2010; 203(2):381–389. [PubMed: 20390256]

Fournier KA, Hass CJ, Naik SK, Lodha N, Cauraugh JH. Motor coordination in autism spectrum disorders: a synthesis and meta-analysis. Journal of autism and developmental disorders. 2010; 40(10):1227–1240. [PubMed: 20195737]

Friedman SD, Shaw DW, Artru AA, Richards TL, Gardner J, Dawson G, et al. Dager SR. Regional brain chemical alterations in young children with autism spectrum disorder. Neurology. 2003; 60(1):100–107. [PubMed: 12525726]

Galaburda AM, Menard MT, Rosen GD. Evidence for aberrant auditory anatomy in developmental dyslexia. Proceedings of the National Academy of Sciences of the United States of America. 1994; 91(17):8010–8013. [PubMed: 8058748]

Gotts SJ, Simmons WK, Milbury LA, Wallace GL, Cox RW, Martin A. Fractionation of social brain circuits in autism spectrum disorders. Brain. 2012; 135(9):2711–2725. [PubMed: 22791801]

Hahamy A, Behrmann M, Malach R. The idiosyncratic brain: distortion of spontaneous connectivity patterns in autism spectrum disorder. Nature neuroscience. 2015; 18(2):302–309. [PubMed: 25599222]

Happé F, Frith U. The weak coherence account: detail-focused cognitive style in autism spectrum disorders. Journal of autism and developmental disorders. 2006; 36(1):5–25. [PubMed: 16450045]

Heaton P. Pitch memory, labelling and disembedding in autism. Journal of Child Psychology and Psychiatry. 2003; 44(4):543–551. [PubMed: 12751846]

Heaton P. Interval and contour processing in autism. Journal of autism and developmental disorders. 2005; 35(6):787–793. [PubMed: 16283085]

Hyde LA, Hoplight BJ, Denenberg VH. Water version of the radial-arm maze: learning in three inbred strains of mice. Brain research. 1998; 785(2):236–244. [PubMed: 9518631]

Jones CR, Happé F, Baird G, Simonoff E, Marsden AJ, Tregay J, et al. Charman T. Auditory discrimination and auditory sensory behaviours in autism spectrum disorders. Neuropsychologia. 2009; 47(13):2850–2858. [PubMed: 19545576]

Kwakye LD, Foss-Feig JH, Cascio CJ, Stone WL, Wallace MT. Altered auditory and multisensory temporal processing in autism spectrum disorders. Frontiers in integrative neuroscience. 2011; 4:129. [PubMed: 21258617]

Lai JK, Sobala-Drozdowski M, Zhou L, Doering LC, Faure PA, Foster JA. Temporal and spectral differences in the ultrasonic vocalizations of fragile × knock out mice during postnatal development. Behavioural brain research. 2014; 259:119–130. [PubMed: 24211451]

Lein ES, Hawrylycz MJ, Ao N, Ayres M, Bensinger A, Bernard A, et al. Jones AR. Genome-wide atlas of gene expression in the adult mouse brain. Nature. 2007; 445(7124):168–176. [PubMed: 17151600]

Li J, Zhao L, You Y, Lu T, Jia M, Yu H, et al. Zhang D. Schizophrenia related variants in CACNA1C also confer risk of autism. PloS one. 2015; 10(7):e0133247. [PubMed: 26204268]

Lein ES, et al. Genome-wide atlas of gene expression in the adult mouse brain. Nature. 2007; 445:168–176. [PubMed: 17151600]

Marco EJ, Hinkley LB, Hill SS, Nagarajan SS. Sensory processing in autism: a review of neurophysiologic findings. Pediatric research. 2011; 69:48R–54R.

Martínez-Sanchis S. Neurobiological foundations of multisensory integration in people with autism spectrum disorders: the role of the medial prefrontal cortex. Frontiers in Human Neuroscience. 2014; 8:970. [PubMed: 25538597]

Michetti C, Ricceri L, Scattoni ML. Modeling social communication deficits in mouse models of autism. Autism-Open Access. 2012; 2012

Moles A, Costantini F, Garbugino L, Zanettini C, D'Amato FR. Ultrasonic vocalizations emitted during dyadic interactions in female mice: a possible index of sociability? Behavioural brain research. 2007; 182(2):223–230. [PubMed: 17336405]

Moreno-De-Luca A, Myers SM, Challman TD, Moreno-De-Luca D, Evans DW, Ledbetter DH. Developmental brain dysfunction: revival and expansion of old concepts based on new genetic evidence. The Lancet Neurology. 2013; 12(4):406–414. [PubMed: 23518333]

Mostofsky SH, Powell SK, Simmonds DJ, Goldberg MC, Caffo B, Pekar JJ. Decreased connectivity and cerebellar activity in autism during motor task performance. Brain. 2009; 132(9):2413–2425. [PubMed: 19389870]

Mottron L, Dawson M, Soulieres I, Hubert B, Burack J. Enhanced perceptual functioning in autism: An update, and eight principles of autistic perception. Journal of autism and developmental disorders. 2006; 36(1):27–43. [PubMed: 16453071]

Mizuno A, Villalobos ME, Davies MM, Dahl BC, Muller R. Partially enhanced thalamocortical functional connectivity in autism. Brain Research. 2006; 1104(1):160–174. [PubMed: 16828063]

Muller R, Chugani DC, Behen ME, Rothermel RD, Muzik O, Chakraborty PK, Chugani HT. Impairment of dentato-thalamo-cortical pathway in autistic men: Language activation data from positron emission tomography. Neuroscience Letters. 1998; 245(1):1–4. [PubMed: 9596341]

Nadler JJ, Moy SS, Dold G, Simmons N, Perez A, Young NB, et al. Crawley JN. Automated apparatus for quantitation of social approach behaviors in mice. Genes, Brain and Behavior. 2004; 3(5):303–314.

Nair A, Treiber JM, Shukla DK, Shih P, MÃ¼ller R. Impaired thalamocortical connectivity in autism spectrum disorder: A study of functional and anatomical connectivity. Brain. 2013; 136(6):1942–1955. [PubMed: 23739917]

O'Riordan MA, Plaisted KC, Driver J, Baron-Cohen S. Superior visual search in autism. Journal of Experimental Psychology: Human Perception and Performance. 2001; 27(3):719. [PubMed: 11424657]

O'Riordan M, Plaisted K. Enhanced discrimination in autism. The Quarterly Journal of Experimental Psychology: Section A. 2001; 54(4):961–979.

Ouimet T, Foster NE, Tryfon A, Hyde KL. Auditory-musical processing in autism spectrum disorders: a review of behavioral and brain imaging studies. Annals of the New York Academy of Sciences. 2012; 1252(1):325–331. [PubMed: 22524375]

Paxinos, G., Watson, C. The rat brain in stereotaxic coordinates. 2nd. San Diego: Academic Press; 1986.

Perreault A, Gurnsey R, Dawson M, Mottron L, Bertone A. Increased sensitivity to mirror symmetry in autism. PLoS One. 2011; 6(4):e19519. [PubMed: 21559337]

Penagarikano O, Abrahams BS, Herman EI, Winden KD, Gdalyahu A, Dong H, Sonnenblick LI, Gruver R, Almajano J, Bragin A, Golshani P, Trachtenberg JT, Peles E, Geschwind DH. Absence of *CNTNAP2* Leads to Epilepsy, Neuronal Migration Abnormalities, and Core Autism-Related Deficits. Cell. 2011; 147:235–246. [PubMed: 21962519]

Penagarikano O, Geschwind D. What does *CNTNAP2* reveal about autism spectrum disorder? Trends in Molecular Medicine. 2012; 18:156–163. [PubMed: 22365836]

Plaisted K, O'Riordan M, Baron-Cohen S. Enhanced visual search for a conjunctive target in autism: A research note. Journal of Child Psychology and Psychiatry. 1998; 39(05):777–783. [PubMed: 9690940]

Plaisted K, O'Riordan M, Baron-Cohen S. Enhanced discrimination of novel, highly similar stimuli by adults with autism during a perceptual learning task. Journal of Child Psychology and Psychiatry. 1998; 39(5):765–775. [PubMed: 9690939]

Plaisted K, Saksida L, Alcántara J, Weisblatt E. Towards an understanding of the mechanisms of weak central coherence effects: Experiments in visual configural learning and auditory perception. Philosophical Transactions of the Royal Society B: Biological Sciences. 2003; 358(1430):375–386.

Poliak S, Salomon D, Elhanany H, Sabanay H, Kiernan B, Pevny L, et al. Furley AJ. Juxtaparanodal clustering of Shaker-like K+ channels in myelinated axons depends on Caspr2 and TAG-1. The Journal of cell biology. 2003; 162(6):1149–1160. [PubMed: 12963709]

Poustka L, Jennen-Steinmetz C, Henze R, Stieltjes B. Fronto-temporal disconnectivity and symptom severity in autism spectrum disorders. The World Journal of Biological Psychiatry. 2012; 13:269–280. [PubMed: 21728905]

Rendall AR, Tarkar A, Contreras-Mora HM, LoTurco JJ, Fitch RH. Deficits in learning and memory in mice with a mutation of the candidate dyslexia susceptibility gene Dyx1c1. Brain and Language. 2015 S0093–934X(15)00102–9.

Rendall AR, Truong DT, Fitch RH. Learning delays in a mouse model of Autism Spectrum Disorder. Behavioural Brain Research. 2016; 303:201–207. [PubMed: 26873041]

Rosenberg RE, Law JK, Yenokyan G, McGready J, Kaufmann WE, Law PA. Characteristics and concordance of autism spectrum disorders among 277 twin pairs. Archives of pediatrics & adolescent medicine. 2009; 163(10):907–914. [PubMed: 19805709]

Russo N, Foxe JJ, Brandwein AB, Altschuler T, Gomes H, Molholm S. Multisensory processing in children with autism: high-density electrical mapping of auditory–somatosensory integration. Autism Research. 2010; 3(5):253–267. [PubMed: 20730775]

Simmons DR, Robertson AE, McKay LS, Toal E, McAleer P, Pollick FE. Vision in autism spectrum disorders. Vision research. 2009; 49(22):2705–2739. [PubMed: 19682485]

Splawski I, Timothy KW, Sharpe LM, Decher N, Kumar P, Bloise R, et al. Tager-Flusberg H. Ca v 1.2 calcium channel dysfunction causes a multisystem disorder including arrhythmia and autism. Cell. 2004; 119(1):19–31. [PubMed: 15454078]

Steffenburg S, Gillberg C, Hellgren L, et al. A twin study of autism in Denmark, Finland, Iceland, Norway and Sweden. Journal of Child Psychology and Psychiatry. 1989; 30(3):405–416. [PubMed: 2745591]

Stewart ME, Griffiths TD, Grube M. Autistic Traits and Enhanced Perceptual Representation of Pitch and Time. Journal of autism and developmental disorders. 2015:1–9. [PubMed: 25428291]

Szalkowski CE, Booker AB, Truong DT, Threlkeld SW, Rosen GD, Fitch RH. Knockdown of the candidate dyslexia susceptibility gene homolog Dyx1c1 in rodents: Effects on auditory processing, visual attention, and cortical and thalamic anatomy. Developmental neuroscience. 2013; 35(1):50–68. [PubMed: 23594585]

Szalkowski CE, Fiondella CG, Galaburda AM, Rosen GD, LoTurco JJ, Fitch RH. Neocortical disruption and behavioral impairments in rats following in utero RNAi of candidate dyslexia risk gene Kiaa0319. International Journal of Developmental Neuroscience. 2012; 30(4):293–302. [PubMed: 22326444]

Tamura R, Kitamura H, Endo T, Hasegawa N, Someya T. Reduced thalamic volume observed across different subgroups of autism spectrum disorders. Psychiatry Research: Neuroimaging. 2010; 184(3):186–188. [PubMed: 20850279]

Travers BG, Adluru N, Ennis C, Tromp DP, Destiche D, Doran S, et al. Alexander AL. Diffusion tensor imaging in autism spectrum disorder: a review. Autism Research. 2012; 5(5):289–313. [PubMed: 22786754]

Truong DT, Che A, Rendall AR, Szalkowski CE, LoTurco JJ, Galaburda AM, Holly Fitch R. Mutation of Dcdc2 in mice leads to impairments in auditory processing and memory ability. Genes, Brain and Behavior. 2014; 13(8):802–811.

Truong DT, Rendall AR, Castelluccio BC, Eigsti IM, Fitch RH. Auditory processing and morphological anomalies in medial geniculate nucleus of *Cntnap2* mutant mice. Behavioral neuroscience. 2015; 129(6):731–743. [PubMed: 26501174]

Tsatsanis KD, Rourke BP, Klin A, Volkmar FR, Cicchetti D, Schultz RT. Reduced thalamic volume in high-functioning individuals with autism. Biological Psychiatry. 2003; 53(2):121–129. [PubMed: 12547467]

Wang H, Liang S, Burgdorf J, Wess J, Yeomans J. Ultrasonic vocalizations induced by sex and amphetamine in M2, M4, M5 muscarinic and D2 dopamine receptor knockout mice. PloS one. 2008; 3(4):e1893. [PubMed: 18382674]

Wen Y, Alshikho MJ, Herbert MR. Pathway Network Analyses for Autism Reveal Multisystem Involvement, Major Overlaps with Other Diseases and Convergence upon MAPK and Calcium Signaling. PloS one. 2016; 11(4):e0153329. [PubMed: 27055244]

Wittkowski KM, Sonakya V, Bigio B, Tonn MK, Shic F, Ascano M, et al. Gold-Von Simson G. A novel computational biostatistics approach implies impaired dephosphorylation of growth factor receptors as associated with severity of autism. Translational psychiatry. 2014; 4(1):e354. [PubMed: 24473445]

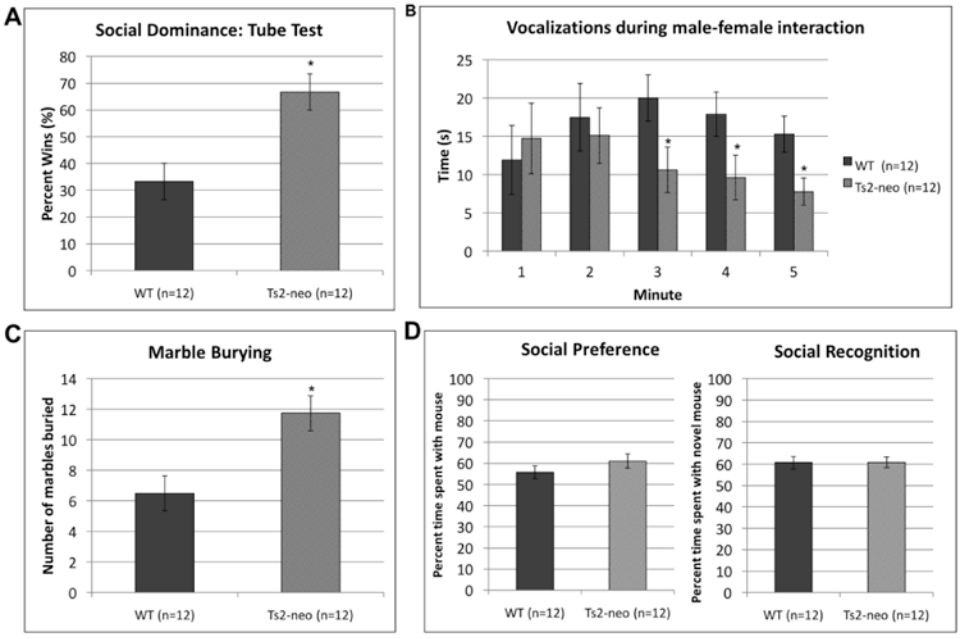

Figure 1. TS2-neo mice display "ASD-like" behavioral profiles

(a.) Social Dominance: TS2-neo mice won significantly more trials on a tube test. (b.) Ultrasonic vocalizations during male-female interactions: TS2-neo mice vocalized significantly less during the last 3 minutes of interaction (c.) Marble burying: TS2-neo mice buried significantly more marbles.

*p<.05

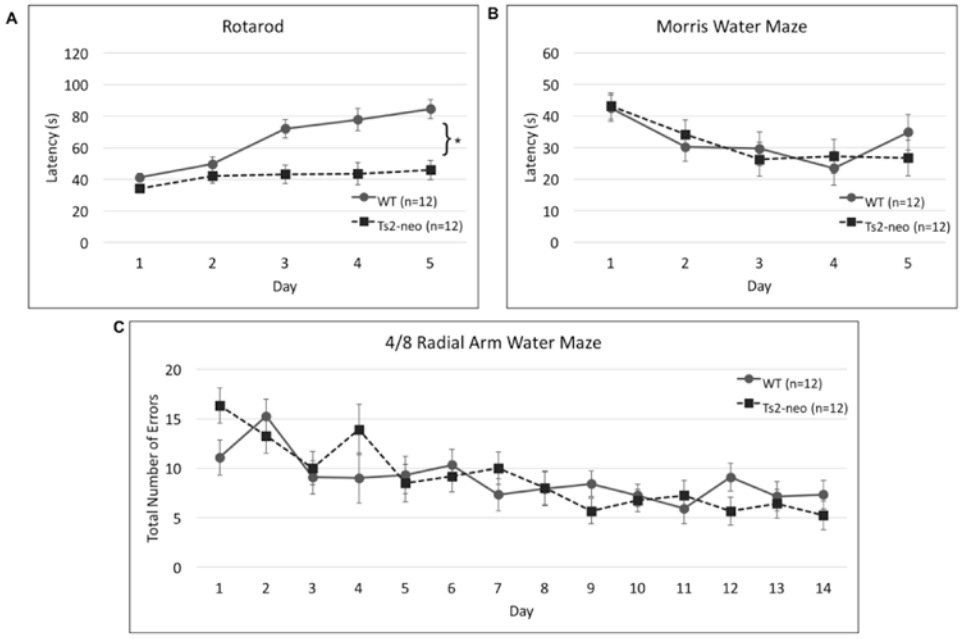

Figure 2. TS2-neo mice show deficits in motor learning but not spatial learning

(a.) Rotarod: TS2-neo mice displayed a lack of motor learning. (b.) Morris Water Maze: TS2-neo mice and WTs performed comparably. (c.) 4/8 Radial Arm Water Maze: TS2-neo mice and WTs displayed similar learning curves on this complex spatial task.

*p<.05

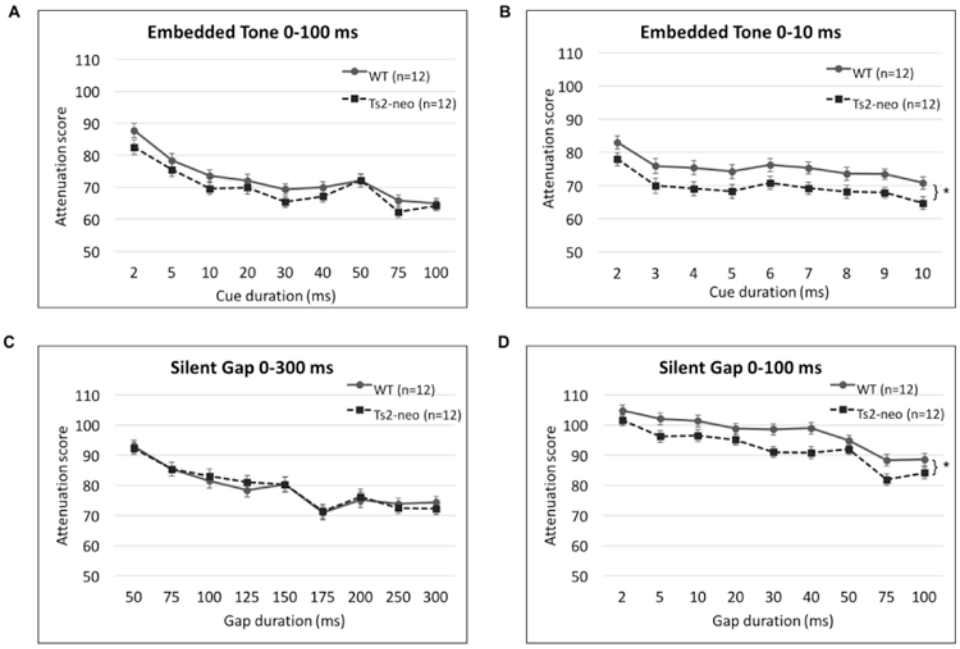

Figure 3. TS2-neo mice exhibit superior processing of short-duration acoustic stimuli

(a.) Embedded Tone 0-100 ms: TS2-neo mice and WTs showed comparable performance. (b.) Embedded Tone 0-10ms: TS2-neo mice had significantly lower (better) attenuation scores. (c.) Silent Gap 0-300 ms: TS2-neo mice and WTs had comparable performance. (d.) Silent Gap 0-100 ms: TS2-neo mice had significantly lower (better) attenuation scores. *p<.05

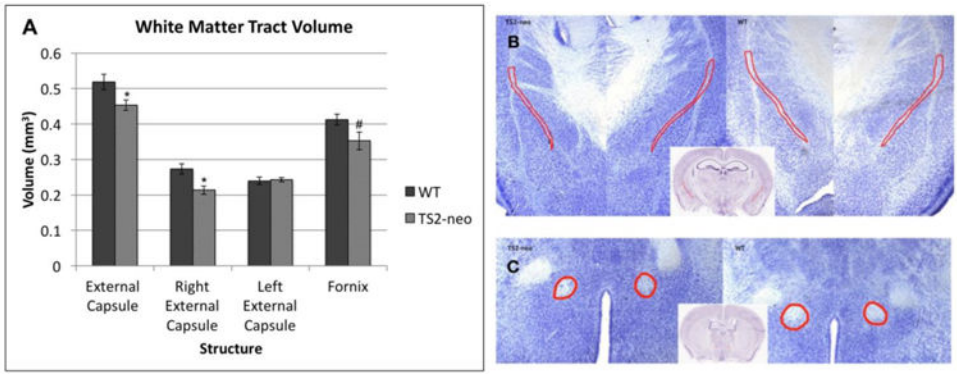

Figure 4. TS2-neo mice show significant decrease in white matter structures

(a.) TS2-neo mice displayed a significant decrease in volume of the external capsule, specifically right external capsule, and a marginal decrease in the fornix. (b.) Location and size of external capsule (outlined in red) for representative TS2-neo and WT samples. (c.) Location and size of fornix (outlined in red) for representative TS2-neo and WT samples. * p<.05, # p=.059

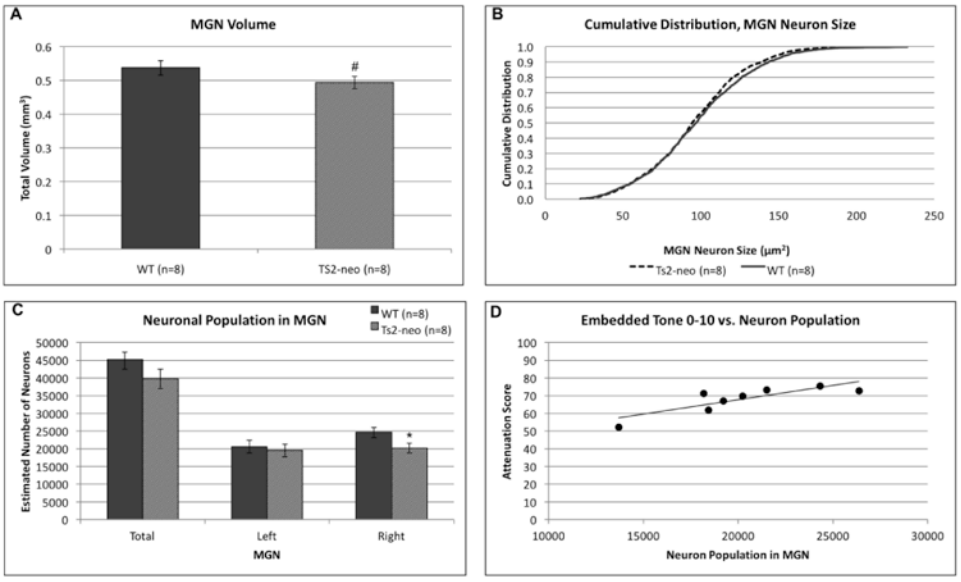

Figure 5. TS2-neo mice display anomalies in the medial geniculate nucleus

(a.) TS2-neo mice exhibit a marginally significant reduction in MGN volume. (b.) TS2-neo display a significant shift in cumulative MGN cell size distribution, with mutants showing more small and fewer large MGN cells compared to WTs. (c.) TS2-neo display reductions in number of MGN neurons, specifically within the right MGN. (d.) A significant positive correlation was revealed between EBT10 attenuation scores and number of neurons in MGN.

* $p<.05$, # $p=.058$